Atmospheric Environment 77 (2013) 927–934

Contents lists available at SciVerse ScienceDirect

Atmospheric Environment

journal homepage: www.elsevier.com/locate/atmosenv

The impact of relative humidity on aerosol composition and evolution processes during wintertime in Beijing, China

Yele Sun [a,*], Zifa Wang [a], Pingqing Fu [a], Qi Jiang [b,a], Ting Yang [a], Jie Li [a], Xinlei Ge [c]

[a] State Key Laboratory of Atmospheric Boundary Layer Physics and Atmospheric Chemistry, Institute of Atmospheric Physics, Chinese Academy of Sciences, Beijing 100029, China
[b] Key Laboratory for Aerosol-Cloud-Precipitation of China Meteorological Administration, Nanjing University of Information Science & Technology, Nanjing 210044, China
[c] Department of Environmental Toxicology, University of California, One Shields Avenue, Davis, CA 95616, USA

HIGHLIGHTS

- The RH impacts on aerosol composition and processes in Beijing were examined.
- The RH shows the largest impact on sulfate and coal combustion OA during wintertime.
- Aqueous processing appears not to significantly enhance SOA production and oxidation degree.

ARTICLE INFO

Article history:
Received 12 April 2013
Received in revised form
5 June 2013
Accepted 10 June 2013

Keywords:
ACSM
Relative humidity
Aqueous-phase production
Organic aerosol
Wintertime
Beijing

ABSTRACT

Non-refractory submicron aerosol (NR-PM_1) species measured by an Aerodyne Aerosol Chemical Speciation Monitor (ACSM) along with collocated gaseous species are used to investigate the impacts of relative humidity (RH) on aerosol composition and evolution processes during wintertime in Beijing, China. Aerosol species exhibit strong, yet different RH dependence between low and high RH levels. At low RH levels (<50%), all aerosol species increase linearly as a function of RH, among which organics present the largest mass increase rate at 11.4 μg m^{-3}/10% RH. Because the particle liquid water predicted by E-AIM model is very low and the temperature is relatively constant, the enhancement of aerosol species is primarily due to the decrease of wind speed. While the rates of increase for most aerosol species are reduced at high RH levels (>50%), sulfate presents an even faster increasing rate, indicating the significant impact of liquid water on sulfate production. The RH dependence of organic aerosol (OA) components is also quite different. Among OA components, coal combustion OA (CCOA) presents the largest enhancement in both mass concentration and contribution as a function of RH. Our results elucidate the important roles of liquid water in aerosol processing at elevated RH levels, in particular affecting sulfate and CCOA via aqueous-phase reaction and gas-particle partitioning associated with water uptake, respectively. It is estimated that aqueous-phase processing can contribute more than 50% of secondary inorganic species production along with an increase of aerosol particle acidity during the fog periods. However, it appears not to significantly enhance secondary organic aerosol (SOA) formation and the oxidation degree of OA.

1. Introduction

Relative humidity (RH) is a key factor influencing chemical composition, size distributions, and optical properties of aerosol particles (Day et al., 2000; Hallquist et al., 2009) and their associated radiative forcing impacts (Markowicz et al., 2003). RH affects aerosol formation in a number of ways, e.g., aqueous-phase reactions and gas-particle partitioning (Altieri et al., 2008; Hennigan et al., 2008). In particular, the effects of RH on the formation of secondary organic aerosol (SOA) have been investigated through both chamber studies and ambient measurements (Cocker III et al., 2001; Hennigan et al., 2009), yet not well understood because of the very complex functionalities and hygroscopicities of organic compounds.

Organic aerosols (OA) comprise a major fraction of fine particles (Kanakidou et al., 2005; Zhang et al., 2007a). However, current models often have large uncertainties in predicting SOA (Volkamer

* Corresponding author. Tel.: +86 10 82021255; fax: +86 10 62041393.
E-mail address: sunyele@mail.iap.ac.cn (Y. Sun).

1352-2310/$ – see front matter © 2013 Elsevier Ltd. All rights reserved.
http://dx.doi.org/10.1016/j.atmosenv.2013.06.019

et al., 2006), and the model bias increases as a function of relative humidity suggesting a missing source of SOA from aqueous-phase processing (Heald et al., 2011). Indeed, aqueous-phase production of SOA might contribute equivalently to the gas-phase production of SOA (Lim et al., 2010; Ervens et al., 2011). Recently, gas-particle partitioning of water-soluble organic compounds (WSOC) associated with water uptake has been found to be an important pathway for SOA formation (Hennigan et al., 2008). Despite this, the RH dependence of gas-particle partitioning of WSOC may vary significantly at different sites because of different composition and aging properties of OA (Zhang et al., 2012b). Most previous studies investigating RH effects on aerosol chemistry are conducted in summer and few of them are focused in winter. Given that aerosol particle composition, hygroscopic properties, and oxidation degree of OA often have large differences between summer and winter, the RH dependent aerosol formation and evolution processes might be quite different as well in the two seasons.

Fog processing associated with enhanced RH is an important pathway to affect aerosol formation and evolution processes during wintertime. Ge et al. (2012) found that aqueous-phase processing during foggy days likely enhanced SOA formation and the oxidation degree of OA. Similarly, Kaul et al. (2011) observed enhanced SOA concentrations during foggy days, and also more acidic aerosol particles because of the oxidation of SO_2 to sulfate. Enhanced production of secondary inorganic species and increase of aerosol acidity were also observed during fog episodes in Beijing (Sun et al., 2006). Fog episodes occur frequently in the North China Plain during wintertime (Quan et al., 2011; Zhang and Tie, 2011), and several fog episodes were observed in this study. However, knowledge of the evolution of aerosol particles, in particular OA, associated with aqueous-phase processing during foggy days in winter in Beijing is rather limited.

In this work, we present an analysis of two-month measurements of aerosol particle composition during wintertime in Beijing, China. The ambient temperature throughout the study is generally low, ranging from −8 to 12 °C, and the precipitation is rather small except a few light snows during 2nd–7th December, 2011, which provides an ideal opportunity to investigate the RH effects on aerosol processing at low ambient temperatures. Here we examine the RH dependence of aerosol chemistry with a focus on the impacts of RH on aerosol composition, processing, and evolution of OA and its oxidation degree.

2. Experimental

2.1. Sampling

Submicron aerosol particles were measured *in situ* with an Aerodyne Aerosol Chemical Speciation Monitor (ACSM) from 21 November, 2011 to 20 January, 2012 at an urban site in Beijing. The site is located at a secondary-story building (~8 m high) in the Institute of Atmospheric Physics, Chinese Academy of Sciences, which is between the north 3rd and 4th ring road. Collocated gaseous species including CO, O_3, NO and NO_y, and SO_2 were measured simultaneously by various gas analyzers from Thermo Scientific. In addition, the meteorology data including relative humidity, temperature, pressure, wind speed, wind direction, solar radiation and precipitation were obtained from the meteorological tower that is approximately 30 m away from the sampling site. The detailed descriptions of the sampling site and measurements have been given in Sun et al. (2013).

2.2. Data analysis

The mass concentrations and chemical composition of non-refractory submicron aerosol species, including organics, sulfate, nitrate, ammonium and chloride were analyzed with standard ACSM data analysis software (v 1.5.1.1). In particular, a composition dependent collection efficiency (CE) as suggested by Middlebrook et al. (2012) was used to account for ACSM detection efficiency that is mainly caused by the particle bounce effects at the vaporizer (Matthew et al., 2008). The positive matrix factorization (PMF, Paatero and Tapper, 1994) was performed on ACSM OA mass spectra (m/z 12–120) to retrieve potential components with different sources and processes. The results of PMF were further evaluated with an Igor Pro-based PMF Evaluation Tool (PET, v2.06) (Ulbrich et al., 2009). Four OA components were identified including three primary factors, i.e., hydrocarbon-like OA (HOA), cooking OA (COA), and coal combustion OA (CCOA), and one secondary factor, i.e., oxygenated OA (OOA). The four components show distinct mass spectral profiles, time series, and diurnal cycles, suggesting their different source characteristics and processes (Fig. S1). HOA represents a traffic-related primary OA with mass spectrum similar to that of diesel exhaust. COA shows a unique diurnal cycle with prominent peaks appearing at meal times. CCOA comprising the major fraction of OA (33% on average) is characterized by pronounced diurnal cycle with highest concentration occurring at nighttime. OOA with mass spectrum similar to that of oxidized OA is a surrogate of SOA, the mass concentration of which shows a gradual increase from morning to late afternoon, suggesting the formation via photochemical processing during daytime. The detailed investigations of sources and processes of OA components have been given in Sun et al. (2013).

Extend Aerosol Thermodynamics Model (E-AIM, Model II) with aerosol composition data (SO_4^{2-}, NO_3^-, and NH_4^+) from ACSM measurements was used to predict liquid water content (LWC) in this study (Clegg et al., 1998). The LWC was estimated with the formation of solids prohibited because RH during this study was generally low (<80%), the predicted LWC for most of time was close to zero if allowing the formation of solids. Fig. S2 shows the time series of predicted LWC and the correlations between LWC and RH. The LWC is rather low (<0.02 g m^{-3}) below RH = ~50%, indicating the minor roles of aerosol water uptake at low RH levels. However, a significant increase of LWC with increasing RH was observed at RH > ~50%, suggesting the importance of aerosol water at elevated RH levels.

3. Results and discussion

3.1. RH effects on aerosol composition

Fig. 1 shows the variations of mass concentrations and mass fractions of NR-PM_1 species and OA components as a function of RH throughout the study. The mass concentrations of most aerosol species appear to increase linearly as a function of RH, yet the rate of increase appears to be different at low and high RH levels. At low RH levels (LRH < ~50%), organics shows the largest mass increasing rate (11.4 μg m^{-3}/10% RH) among NR-PM_1 species followed by nitrate, ammonium, and sulfate (Table 1). By contrast, the enhancement rates for most aerosol species are reduced by a factor of ~1.3–4.6 at RH > 50%, whereas sulfate shows an even faster increasing rate (6.0 vs. 2.9 μg m^{-3}/10% RH), suggesting the different RH impacts on different aerosol species, and in particular the significant impact on sulfate production. The OA components show a similar RH dependence with faster increasing rates at low RH levels. It's interesting to note that RH shows weaker impacts on primary HOA and COA than OOA and CCOA, likely due to their lower oxidation degree and hygroscopicities (Wong et al., 2011). Fig. S3 shows the variations of meteorological variables as a function of RH. As temperature and pressure are fairly constant across different RH levels, wind speed shows a dramatic decrease at LRH levels, and

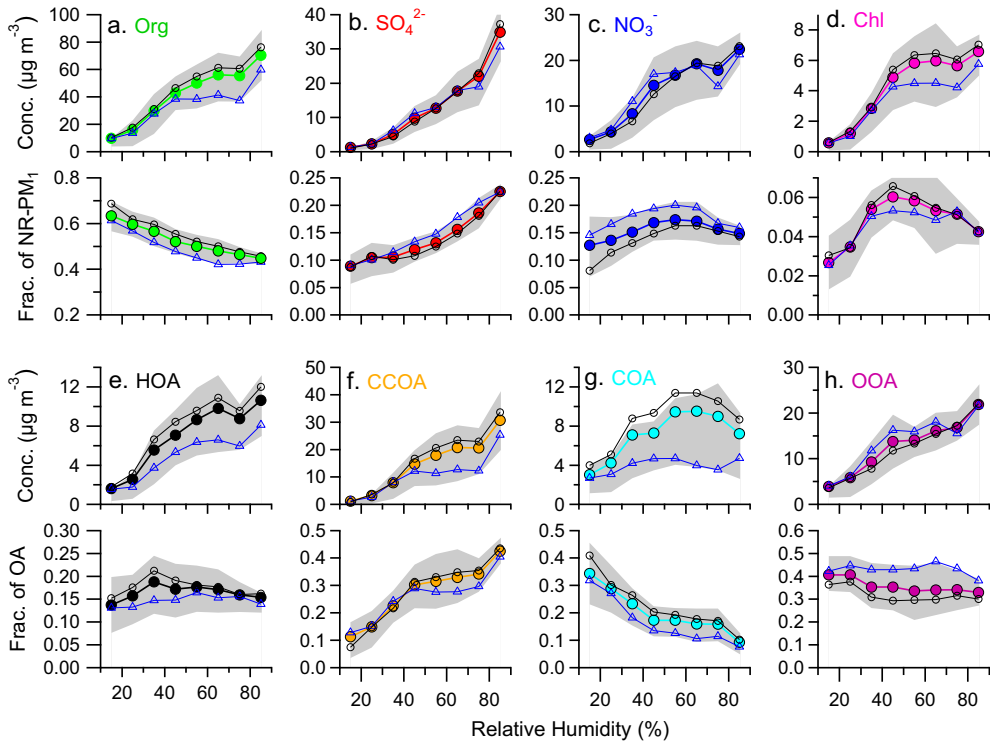

Fig. 1. Variations of mass concentrations and mass fraction of NR-PM$_1$ species and OA components as a function of RH. The data are grouped in RH bins (10% increment). The solid circles refer to the mean values and the shaded areas indicate the 25th and 75th percentiles. The open circles and triangles refer to the average of the data during daytime and nighttime, respectively.

then remains low (<1 m s^{-1}) at RH > 40%. Given that wind is very efficient in cleaning up air pollutants in winter in Beijing (Sun et al., 2013), we conclude that the increase of aerosol species below RH = ~50% is primarily due to the decrease of wind speed. Consistently, the predicted fine particle liquid water at RH < ~50% is generally low (<0.02 g m^{-3}), supporting that aqueous-phase processing could not play significant roles. When the wind effects are not significant at high RH (HRH) levels, the increasing rates are correspondingly slowed down. Note HOA that is expected to be non-hygroscopic is still elevated as the increase of RH, indicating the continuous yet weak accumulation at HRH levels. This is also consistent with the simultaneous enhancements of primary gaseous species, e.g., NO, NO$_y$, and CO. It should be noted that the increasing rates at HRH levels are lower and the variations even appear to be flat if not considering the data at RH > 80%. One explanation is that the aerosol processing at RH > 80% might be different from other HRH levels. In addition to the accumulation processes associated with the stagnant meteorology, aqueous-phase processing, e.g., water-uptake and/or reactions associated with enhanced LWC might also have played a significant role in affecting aerosol composition and evolution at elevated RH periods, for example sulfate (see Section 3.2 for details).

Fig. 2 presents the average chemical composition of NR-PM$_1$ and OA at low and high RH levels for the entire study. The average mass concentration of NR-PM$_1$ at RH > 50% is 113.7 μg m^{-3}, which is almost a factor of 3 of that at RH < 50%. All NR-PM$_1$ species show significant enhancements in mass concentrations by a factor of

Table 1
The average rate of increase (μg m^{-3}/10% RH) of NR-PM$_1$ species and OA components at low RH (<50%) and high RH levels (>50%). The rate of increase was obtained from the linear regression slope of mass concentration vs. RH in Fig. 1.

	Low RH	High RH	L/H ratio
Org	11.4	6.0	1.9
OOA	3.3	1.9	1.7
CCOA	4.6	3.5	1.3
COA	1.6	−0.1	–
HOA	1.9	0.7	2.7
SO_4^{2-}	2.9	6.0	0.5
NO_3^-	4.0	1.7	2.3
NH_4^+	3.0	2.2	1.4
Chl	1.5	0.3	4.6

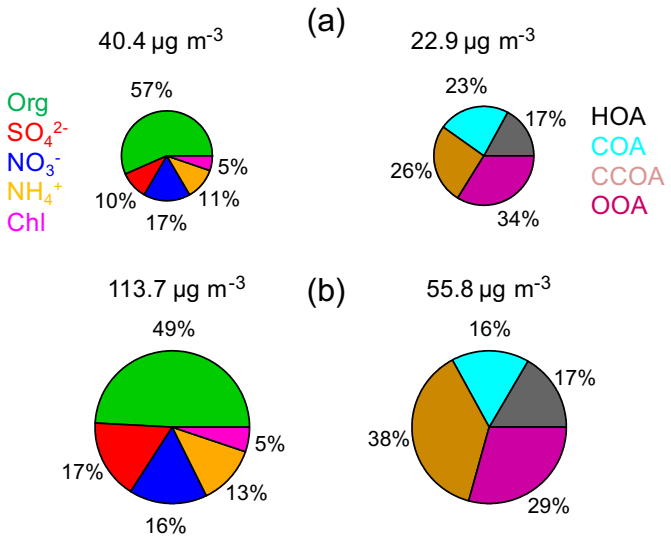

Fig. 2. Average chemical composition of NR-PM$_1$ and OA at (a) low RH (<50%) and (b) high RH (>50%) levels.

more than 2 at elevated RH periods, among which sulfate shows the largest enhancement by a factor of ~5 from 4 to 19 μg m^{-3}. Despite this, organics comprise the dominant fraction of NR-PM_1 at both LRH and HRH levels, contributing 57% and 49%, respectively. While the contribution of nitrate, ammonium, and chloride to NR-PM_1 are close between LRH and HRH levels, the sulfate contribution shows a significant enhancement from 10% to 17%, confirming the largest impact of RH on sulfate production. Similar to NR-PM_1 species, the OA components show synchronous enhancements at high RH levels, of which CCOA shows the largest enhancement by a factor of 3.5 from 6 to 21 μg m^{-3}, whereas the enhancements of other OA components are relatively close, generally by a factor of ~2. The OA composition is quite different between LRH and HRH levels. While the POA dominates OA composition at both LRH and HRH, accounting for 71% and 66%, respectively, CCOA is the only OA component showing an enhancement contribution at high RH levels by 13%, indicating the significance of CCOA in air pollution at elevated RH periods during wintertime. The OOA accounting for approximately one third of OA, however, shows slightly lower contribution at HRH than LRH (34% vs. 29%).

3.2. RH effects on aerosol processing

To evaluate the importance of aqueous-phase processing, all aerosol species are normalized to HOA to exclude the accumulation and/or dilution effects. This approach might have uncertainties since the emissions of HOA are not constant throughout the day. However, such effect might be reduced and insignificant when it is averaged as a function of RH. Fig. 3 shows the variations of the ratios of NR-PM_1 species to HOA as a function of RH. All the ratios were further normalized to the values at RH = 10–20%. As shown in Fig. 3a, the RH appears to show minor impacts on sulfate production below RH = 40%. However, a large enhancement of SO_4^{2-} production, almost by a factor of 5 at RH = 80–90% was observed. Typically, aqueous-phase oxidation of SO_2 is much faster than gas-phase oxidation process (Seinfeld and Pandis, 2006). The oxidation rate in aqueous-phase depends on the droplet pH and the concentrations of oxidants, e.g., hydrogen peroxide, ozone, and oxygen (catalyzed by metals) (Shen et al., 2012). Fig. 3a shows the variation of the fraction of sulfate in total sulfur ($F_{SO_4^{2-}}$, Eq. (1)), which is also known as sulfur oxidation ratio (SOR, Sun et al., 2006), as a function of RH.

$$F_{SO_4^{2-}} = \frac{n\left[SO_4^{2-}\right]}{n\left[SO_4^{2-}\right] + n[SO_2]} \quad (1)$$

where n refers to the molar concentration of SO_4^{2-} and SO_2. Note $F_{SO_4^{2-}}$ calculated here are expected to be lower than those previously calculated with SO_4^{2-} in $PM_{2.5}$ because a considerable fraction of SO_4^{2-} might exist in particles with diameter between 1 and 2.5 μm that ACSM cannot detect. Nevertheless, this would not affect significantly the relationship between $F_{SO_4^{2-}}$ and RH. As shown in Fig. 4a, $F_{SO_4^{2-}}$ presents an evident exponential relationship with RH with minor dependence on temperature. The average $F_{SO_4^{2-}}$ at RH < 40% is less than 0.05, indicating a very low sulfur oxidation ratio. As RH increases, the $F_{SO_4^{2-}}$ rapidly increases and reaches a value of ~0.23 at RH = 80–90%. Because of low solar radiation and O_3 at elevated RH levels (Fig. S3d and i), photochemical production of sulfate is expected to be low. Instead, the aqueous-phase oxidation would play the major role. The aqueous-phase production of sulfate is consistent with the corresponding reduction of SO_2 at HRH levels, in particular beyond RH = 70% with high LWC (Fig. S3e). Similar SO_2 reduction due to aqueous-phase oxidation during fog episodes was also observed previously in the North China Plain (Sun et al., 2006; Zhang and Tie, 2011).

The uptake of SO_2 and further aqueous-phase oxidation could increase aerosol particle acidity. For example, aerosol particles are found to be acidic and cannot be fully neutralized during an intense haze–fog episode in the winter of 2004 in Beijing (Sun et al., 2006). Similarly, ~60% of cloud water samples collected at Mountain Tai in the North China Plain have pH values between 3 and 5, largely due to the rapid oxidation of high concentration of SO_2 in clouds (Shen et al., 2012). In this study, we evaluate the particle acidity by comparing the measured NH_4^+ ($NH_4^+{}_{meas}$) with the predicted NH_4^+ ($NH_4^+{}_{pred}$) needed to fully neutralize SO_4^{2-}, NO_3^- and chloride (Zhang et al., 2007b). The $NH_4^+{}_{pred}$ can be calculated using Eq. (2) as recommended by Zhang et al. (2007b).

$$NH_4^+{}_{pred} = 18 \times \left(2 \times \frac{SO_4^{2-}}{96} + \frac{NO_3^-}{62} + \frac{Chl}{35.5}\right) \quad (2)$$

As shown in Fig. 5, the correlation between $NH_4^+{}_{meas}$ and $NH_4^+{}_{pred}$ shows an evident RH dependence, and the ratio of $NH_4^+{}_{meas}/NH_4^+{}_{pred}$ varies from ~1.01 at RH < 30% to ~0.88 at

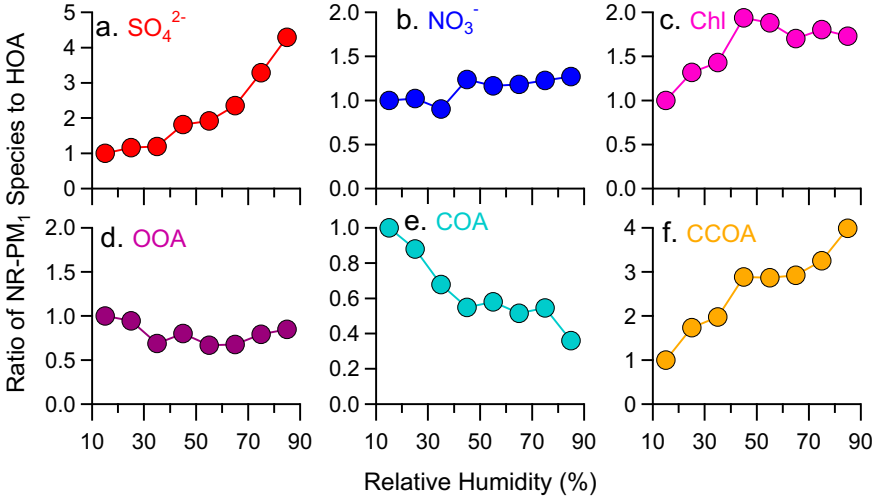

Fig. 3. RH dependence of the ratios of NR-PM_1 species and OA components to HOA. The data are grouped in RH bins (10% inclement). All the ratios are further normalized to the average values between RH = 10–20%.

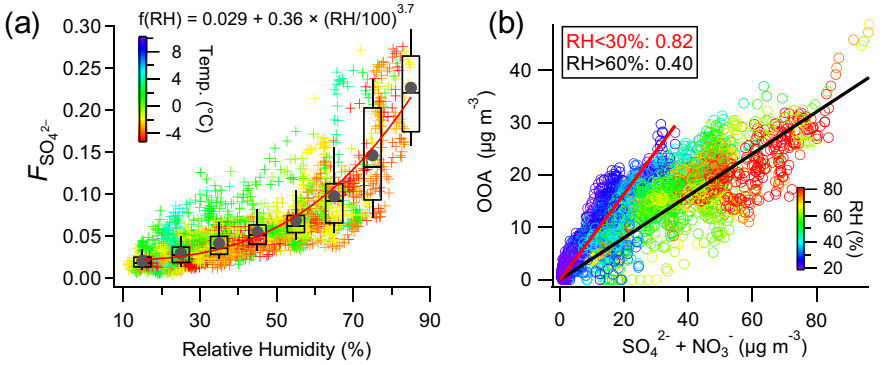

Fig. 4. (a) Relationship between $F_{SO_4^{2-}}$ and RH color coded by temperature. The data are also binned according to RH, and the median (middle horizontal line), mean (solid circles), 25th and 75th percentiles (lower and upper box), and 10th and 90th percentiles (lower and upper whiskers) are shown for each bin. (b) Correlation between OOA and $SO_4^{2-} + NO_3^-$ that is color coded by RH. The regression slope of OOA vs. $SO_4^{2-} + NO_3^-$ for RH < 30% and RH > 60% are also shown. (For interpretation of the references to color in this figure legend, the reader is referred to the web version of this article.)

RH > 60%, suggesting an increase of aerosol acidity as a function of RH due to the aqueous-phase oxidation of SO_2. This is also consistent with the low ambient concentration of NH_3 during wintertime (Ianniello et al., 2011; Meng et al., 2011), which is likely not enough to fully neutralize the newly formed acidic aerosol particles. The HOA-normalized NO_3^- does not present a large increase as SO_4^{2-}, yet ~20–30% enhancement at HRH levels were observed. This suggests that the RH impacts on aqueous-phase production of nitrate during wintertime are limited.

The HOA-normalized OOA shows a quite different RH-dependent behavior from SO_4^{2-}, yet more similar to NO_3^- (Fig. 3d). Although the OOA concentration is elevated by more than 50% from RH = 50%–90%, the HOA-normalized OOA is fairly constant across the high RH levels (Fig. 3d), suggesting that aqueous-phase processing at low ambient temperatures (−8 to 12 °C in this study) appear not to significantly enhance SOA production in submicron aerosols during wintertime in Beijing. This is somewhat different from previous studies in summer in Atlanta, U.S. that a significant enhancement of SOA formation due to water uptake occurred at RH > ~70% (Hennigan et al., 2008). One explanation is that the oxidation degree of SOA in winter is lower than that in summer. The hygroscopicity of SOA is correspondingly low, and gas-particle partitioning associated with liquid water content would be less sensitive. For example, Ge et al. (2012) found an enhancement of SOA production during fog periods in winter in Fresno, CA, yet the enhancement was not significant (~12%). In addition, the wet scavenging or the growth of large OOA particles that ACSM cannot detect under high LWC might also counteract the formation of SOA although it cannot be evaluated in this study.

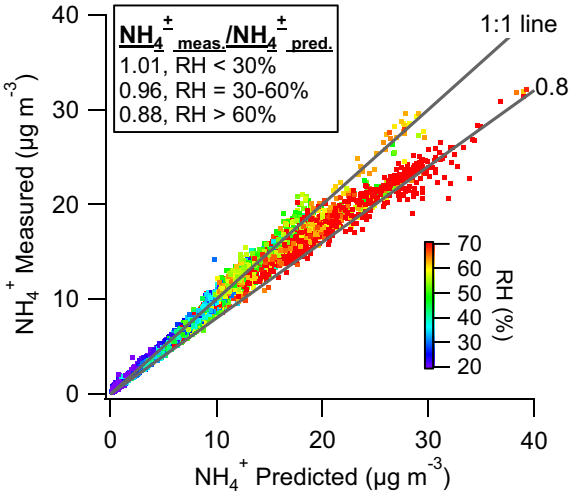

Fig. 5. Correlation between measured NH_4^+ and predicted NH_4^+ (=18 × (2 × SO_4^{2-}/96 + NO_3^-/62 + Chl/35.5)) color coded by RH. The regression slopes at RH < 30%, RH = 30–60%, and RH > 60% are also shown. (For interpretation of the references to color in this figure legend, the reader is referred to the web version of this article.)

Fig. 4b shows the correlation between OOA and the sum of secondary SO_4^{2-} and NO_3^-. OOA shows overall tight correlation with secondary inorganic species (r^2 = 0.75), and the correlation is strongly RH dependent with stronger correlation at lower RH levels (e.g., RH < 20%, r^2 = 0.92, slope = 0.86). While tight correlation continues as the increase of RH, the slope ratio of OOA/($SO_4^{2-} + NO_3^-$), however, decreases gradually from 0.82 at RH < 30% to 0.40 at RH > 60%. In fact, the value of 0.40 at RH > 60% is close to that observed in summer when RH is generally high (Sun et al., 2010, 2012). These results suggest the different impacts of RH on processing SOA and secondary inorganic species. Given the relatively small influences of aqueous-phase processing on SOA production in this study, the decrease of OOA/($SO_4^{2-} + NO_3^-$) is therefore primarily due to the increased production of secondary inorganic species. Also note that the particle phase water at low RH levels (<30%) is negligible, thus the aqueous-phase production of secondary species is expected to be small, and the secondary inorganic sulfate and nitrate would be dominantly from photochemical production (Khoder, 2002). If assuming that the ratio of OOA/($SO_4^{2-} + NO_3^-$) associated with photochemical processing is constant across different RH levels, we can estimate the relative contribution of aqueous-phase production using Eq. (3).

$$SN_{aq} = SN_{total} - OOA \times \left(\frac{SN}{OOA}\right)_{LRH} \quad (3)$$

where SN refers to the sum of sulfate and nitrate, and $(SN/OOA)_{LRH}$ is the slope ratio of SN to OOA at LRH (<30%). Using this approach, we estimate that aqueous-phase production could contribute ~50% for the enhancement of secondary inorganic species at elevated RH levels (>60%) during wintertime. Also note that the RH-dependent relationship between OOA and NO_3^- is weaker than that between OOA and SO_4^{2-} (Fig. S4), consistent with the lower RH dependence of nitrogen oxidation ratio ($F_{NO_3^-} = n[NO_3^-]/n[NO_3^-]+n[NO_2]$, n refers to molar concentration) than $F_{SO_4^{2-}}$ (Fig. S5). Results here further illustrate that aqueous-phase processing contributes differently to the enhancement of sulfate and nitrate at elevated RH levels. Based on Eq. (3) and the correlations of OOA vs. sulfate, and OOA vs. nitrate (Fig. S4), we estimate that aqueous-phase

processing accounts for ~70% of sulfate production at RH > 60%, while <30% for the nitrate formation, which suggests that aqueous-phase processing plays a more important role in production of sulfate than nitrate. Although aqueous processing also played a role in nitrate formation during wintertime, it appears not as significant as that of photochemical production (Sun et al., 2013).

The HOA-normalized CCOA and chloride show similar and large enhancements as a function of RH (Fig. 3c and f), and such enhancements are more significant below RH < 50%. Previous work found that oxygenated compounds comprise a major fraction of quantified organic species in the emissions of coal combustion from industrial boilers, with 46–68% being organic acids (Zhang et al., 2008). Therefore, high RH and liquid water that facilitates gas-particle partitioning of semi-volatile WSOC might be the major reason for the enhancement of CCOA. A recent study in Los Angeles also observed an enhanced partitioning of soluble WSOC below RH = 60% (Zhang et al., 2012b). In addition, the increased organic mass at high RH might also serve as an absorbing phase and enhance the partitioning of WSOC (Zhang et al., 2012b). Similarly, the increase of chloride as a function of RH is also likely due to gas-particle partitioning associated with elevated particle liquid water. Coal combustion is an important source of chloride during wintertime in Beijing. Zhang et al. (2012a) found a molar ratio of 1.3 (mass ratio ≈0.24) for NH_4^+/SO_4^{2-} from coal combustion, which is lower than 2.0 that is needed to fully neutralize sulfate. This indicates that aerosol particles from coal combustion are acidic. As a result, chloride may exist partially in the form of HCl, which can readily partition to aqueous-phase and increase the aerosol acidity as well.

RH also exerts different impacts on processing primary and secondary species between daytime and nighttime (Fig. 1). The secondary species (SO_4^{2-}, NO_3^-, and OOA) shows small day–night differences as a function of RH, yet a slight enhancement of NO_3^- and OOA mass between RH = 30–70% during daytime due to photochemical processing (Fig. 1c and h). Such a daytime enhancement is more evident in terms of the mass contributions of NO_3^- and OOA to NR-PM_1 and OA, respectively. The NO_3^- and OOA exhibit small day–night differences at RH > 70%, likely due to the weak photochemical processing associated with the reduced solar radiation and low O_3 level (Fig. S3d and i). While the primary species, e.g., CCOA and chloride, show relatively small day–night differences at low RH levels, the differences are significantly enlarged at high RH levels, e.g., HOA and CCOA owing to the much enhanced primary emissions at nighttime (Sun et al., 2013).

3.3. RH effects on organic aerosol evolution

We further examined the impact of RH on the evolution of OA during wintertime. Fig. 6a shows the variations of the signal fractions of three AMS *m/z*'s (*m/z* 44, 43, and 57) in OA, i.e., *f*44, *f*43, and *f*57 as a function of RH. *m/z* 44 (mostly CO_2^+) and *m/z* 57 (mostly $C_4H_9^+$ at urban sites) have been widely used as AMS spectral tracers for OOA, a surrogate of secondary OA, and HOA, a surrogate of primary OA from fuel combustion emissions, respectively (Zhang et al., 2005; Ng et al., 2011). *f*44 is also used to elucidate the aging processes because of its tight correlation with the oxidation degree (oxygen-to-carbon, O/C) of OA (Aiken et al., 2008). For example, the highly oxidized low-volatility OOA (LV-OOA) shows much higher *f*44 than less oxidized semi-volatile OOA (SV-OOA) (0.17 ± 0.04 vs. 0.07 ± 0.04) (Ng et al., 2010). However, *m/z* 43 (mostly $C_3H_7^+$ and $C_2H_3O^+$) has been observed to be a major fragment of SV-OOA, and f_{43} can be used to indicate the semi-volatile properties of OA (Ng et al., 2010). The aging of OA leads to an increase of *f*44 and hygroscopicity, and a decrease of *f*43 and volatility (Jimenez et al., 2009; Ng et al., 2010). In this study, *f*44 decreases from ~0.14 to ~0.09 when RH varies from 10% to 50%, and then remains fairly constant at RH > 50%. In contrast, *f*57 shows a reversed trend as *f*44. Considering the enhancement of organic mass loading as a function of RH below 50%, results here suggest less oxygenated materials at higher organic mass loading. Further, the dilution processes appear to increase the oxidation degree of OA while decrease its mass loading at the same time. Such mass loading dependent oxidation degree of OA have been observed in a number of previous studies (Jimenez et al., 2009; Shilling et al., 2009; DeCarlo et al., 2010). We also note that the contribution of POA to OA is slightly elevated at RH < 50%, which might explain somewhat the decrease of oxidation degree of OA. *f*44 and *f*57 exhibit minor variations at high RH levels, suggesting that aqueous-phase processing does not change the oxidation degree of OA significantly in this study. Yet, higher *f*44 and lower *f*57 during daytime were observed, indicating that aqueous-phase processing in the presence of solar radiation enhance the oxidation degree of OA. Although previous studies suggest that fog processing could enhance the oxidation degree of OA (Ge et al., 2012) and high RH

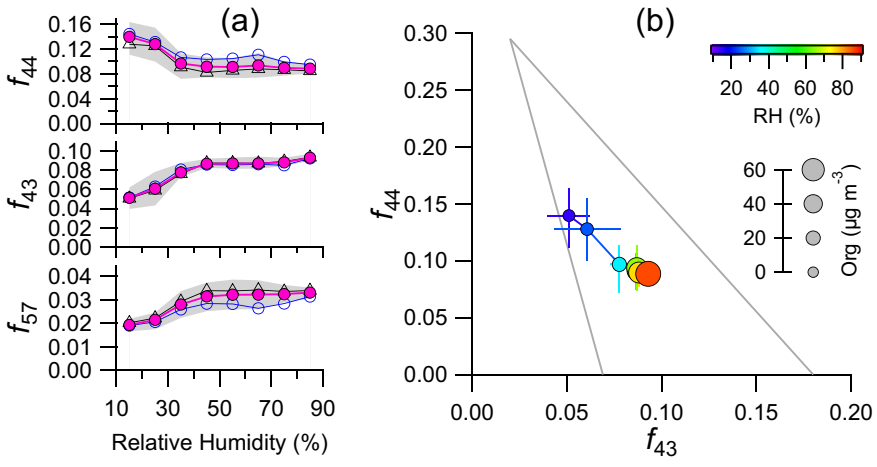

Fig. 6. Variations of *f*44, *f*43, and *f*57 as a function of RH. The data are grouped in RH bin (10% increment). The solid circles are the mean values, and the shaded areas indicate 25th and 75th percentiles. The open circles and triangles are the mean values of daytime and nighttime, respectively. (b) Relationship between *f*44 and *f*43 color coded by RH. The data are binned according to RH (10% increment). The 25th (left and bottom) and 75th (right and top) percentiles are also shown. The marker sizes are proportional to the mass concentrations of organics. (For interpretation of the references to color in this figure legend, the reader is referred to the web version of this article.)

also leads to enrichment of oxygenated species, in particular organic acids (Sorooshian et al., 2010), our results appear not to show such RH effects. This might be due to the competing effects of the formation of small molecular weight products (e.g., organic acids) with high oxidation degree, and oligomers with high molecular weight, yet low oxidation degree (Altieri et al., 2008), leading to a minor effect on overall oxidation degree of OA. The evolution of OA as a function of RH is further illustrated in the triangle plot (*f*44 vs. *f*43) in Fig. 6b (Ng et al., 2010). As RH increases, the OA evolves from the top region to the bottom of the triangle in accompany with a decrease of *f*44 and increase of *f*43, suggesting an evident evolution process from more oxidized to less aged OA.

4. Conclusions

The impacts of RH on aerosol composition and processing during wintertime have been examined in this study. Most aerosol species exhibit strong yet different RH dependence, leading to significantly different submicron aerosol composition between low and high RH levels. While OA comprises the major fraction of NR-PM_1 across different RH levels, sulfate shows the largest increase of the contribution to NR-PM_1 from 10% at RH $<$ 50% to 17% at RH $>$ 50%. Among OA components, CCOA presents the largest enhancement as a function of RH. At elevated RH levels, aqueous-phase processing plays a more significant role, particularly affecting sulfate and CCOA, in comparison to the dominant accumulation processes associated with the decrease of wind speed at low RH levels. It's estimated that fog processing of SO_2 could contribute $\sim$70% of sulfate production during wintertime in Beijing, by contrast aqueous-phase production accounts for $<$30% for the nitrate formation. Although aqueous-phase production contributes significantly to secondary inorganic species and increases the aerosol particle acidity, it appears not to enhance SOA production significantly as previous study reported. Further, aqueous-phase processing does not change much the oxidation degree of OA, yet higher oxidation degree during daytime because of aqueous-phase processing in the presence of solar radiation was observed. Our results suggest that RH has different impacts on processing organic and inorganic aerosols at low ambient temperatures during wintertime. In particular, the RH shows the most impact on sulfate and CCOA at elevated RH periods, which has significant implications that priority should be taken to control the emissions of SO_2 and coal combustion for mitigation of air pollution in haze–fog episodes during wintertime in Beijing, China.

Acknowledgments

This work was supported by the Strategic Priority Research Program (B) of the Chinese Academy of Sciences (Grant No. XDB05020501), the National Key Project of Basic Research (2013CB955801), and the National Natural Science Foundation of China (41175108). We thank Huabin Dong for providing the gaseous species data and the Technical and Service Center, Institute of Atmospheric Physics, Chinese Academy of Sciences for the meteorology data.

Appendix A. Supplementary data

Supplementary data related to this article can be found at http://dx.doi.org/10.1016/j.atmosenv.2013.06.019.

References

Aiken, A.C., DeCarlo, P.F., Kroll, J.H., Worsnop, D.R., Huffman, J.A., Docherty, K.S., Ulbrich, I.M., Mohr, C., Kimmel, J.R., Sueper, D., Sun, Y., Zhang, Q., Trimborn, A., Northway, M., Ziemann, P.J., Canagaratna, M.R., Onasch, T.B., Alfarra, M.R., Prevot, A.S.H., Dommen, J., Duplissy, J., Metzger, A., Baltensperger, U., Jimenez, J.L., 2008. O/C and OM/OC ratios of primary, secondary, and ambient organic aerosols with high-resolution time-of-flight aerosol mass spectrometry. Environ. Sci. Technol. 42, 4478–4485.

Altieri, K.E., Seitzinger, S.P., Carlton, A.G., Turpin, B.J., Klein, G.C., Marshall, A.G., 2008. Oligomers formed through in-cloud methylglyoxal reactions: chemical composition, properties, and mechanisms investigated by ultra-high resolution FT-ICR mass spectrometry. Atmos. Environ. 42, 1476–1490.

Clegg, S.L., Brimblecombe, P., Wexler, A.S., 1998. A thermodynamic model of the system H^+-NH_4^+-SO_4^{2-}-NO_3^--H_2O at tropospheric temperatures. J. Phys. Chem. A 102, 2137–2154.

Cocker III, D.R., Clegg, S.L., Flagan, R.C., Seinfeld, J.H., 2001. The effect of water on gas–particle partitioning of secondary organic aerosol. Part I: α-pinene/ozone system. Atmos. Environ. 35, 6049–6072. http://dx.doi.org/10.1016/s1352-2310(01)00404-6.

Day, D.E., Malm, W.C., Kreidenweis, S.M., 2000. Aerosol light scattering measurements as a function of relative humidity. J. Air Waste Manag. Assoc. 50, 710–716.

DeCarlo, P.F., Ulbrich, I.M., Crounse, J., de Foy, B., Dunlea, E.J., Aiken, A.C., Knapp, D., Weinheimer, A.J., Campos, T., Wennberg, P.O., Jimenez, J.L., 2010. Investigation of the sources and processing of organic aerosol over the Central Mexican Plateau from aircraft measurements during MILAGRO. Atmos. Chem. Phys. 10, 5257–5280. http://dx.doi.org/10.5194/acp-10-5257-2010.

Ervens, B., Turpin, B.J., Weber, R.J., 2011. Secondary organic aerosol formation in cloud droplets and aqueous particles (aqSOA): a review of laboratory, field and model studies. Atmos. Chem. Phys. 11, 11069–11102. http://dx.doi.org/10.5194/acp-11-11069-2011.

Ge, X., Zhang, Q., Sun, Y., Ruehl, C.R., Setyan, A., 2012. Effect of aqueous-phase processing on aerosol chemistry and size distributions in Fresno, California, during wintertime. Environ. Chem. 9, 221–235.

Hallquist, M., Wenger, J.C., Baltensperger, U., Rudich, Y., Simpson, D., Claeys, M., Dommen, J., Donahue, N.M., George, C., Goldstein, A.H., Hamilton, J.F., Herrmann, H., Hoffmann, T., Iinuma, Y., Jang, M., Jenkin, M.E., Jimenez, J.L., Kiendler-Scharr, A., Maenhaut, W., McFiggans, G., Mentel, T.F., Monod, A., Prevot, A.S.H., Seinfeld, J.H., Surratt, J.D., Szmigielski, R., Wildt, J., 2009. The formation, properties and impact of secondary organic aerosol: current and emerging issues. Atmos. Chem. Phys. 9, 5155–5235.

Heald, C.L., Coe, H., Jimenez, J.L., Weber, R.J., Bahreini, R., Middlebrook, A.M., Russell, L.M., Jolleys, M., Fu, T.M., Allan, J.D., Bower, K.N., Capes, G., Crosier, J., Morgan, W.T., Robinson, N.H., Williams, P.I., Cubison, M.J., DeCarlo, P.F., Dunlea, E.J., 2011. Exploring the vertical profile of atmospheric organic aerosol: comparing 17 aircraft field campaigns with a global model. Atmos. Chem. Phys. 11, 12673–12696. http://dx.doi.org/10.5194/acp-11-12673-2011.

Hennigan, C.J., Bergin, M.H., Dibb, J.E., Weber, R.J., 2008. Enhanced secondary organic aerosol formation due to water uptake by fine particles. Geophys. Res. Lett. 35, L18801. http://dx.doi.org/10.1029/12008GL035046.

Hennigan, C.J., Bergin, M.H., Russell, A.G., Nenes, A., Weber, R.J., 2009. Gas/particle partitioning of water-soluble organic aerosol in Atlanta. Atmos. Chem. Phys. 9, 3613–3628.

Ianniello, A., Spataro, F., Esposito, G., Allegrini, I., Hu, M., Zhu, T., 2011. Chemical characteristics of inorganic ammonium salts in PM2.5 in the atmosphere of Beijing (China). Atmos. Chem. Phys. 11, 10803–10822. http://dx.doi.org/10.5194/acp-11-10803-2011.

Jimenez, J.L., Canagaratna, M.R., Donahue, N.M., Prevot, A.S.H., Zhang, Q., Kroll, J.H., DeCarlo, P.F., Allan, J.D., Coe, H., Ng, N.L., Aiken, A.C., Docherty, K.S., Ulbrich, I.M., Grieshop, A.P., Robinson, A.L., Duplissy, J., Smith, J.D., Wilson, K.R., Lanz, V.A., Hueglin, C., Sun, Y.L., Tian, J., Laaksonen, A., Raatikainen, T., Rautiainen, J., Vaattovaara, P., Ehn, M., Kulmala, M., Tomlinson, J.M., Collins, D.R., Cubison, M.J., Dunlea, E.J., Huffman, J.A., Onasch, T.B., Alfarra, M.R., Williams, P.I., Bower, K., Kondo, Y., Schneider, J., Drewnick, F., Borrmann, S., Weimer, S., Demerjian, K., Salcedo, D., Cottrell, L., Griffin, R., Takami, A., Miyoshi, T., Hatakeyama, S., Shimono, A., Sun, J.Y., Zhang, Y.M., Dzepina, K., Kimmel, J.R., Sueper, D., Jayne, J.T., Herndon, S.C., Trimborn, A.M., Williams, L.R., Wood, E.C., Middlebrook, A.M., Kolb, C.E., Baltensperger, U., Worsnop, D.R., 2009. Evolution of organic aerosols in the atmosphere. Science 326, 1525–1529. http://dx.doi.org/10.1126/science.1180353.

Kanakidou, M., Seinfeld, J.H., Pandis, S.N., Barnes, I., Dentener, F.J., Facchini, M.C., Dingenen, R.V., Ervens, B., Nenes, A., Nielsen, C.J., Swietlicki, E., Putaud, J.P., Balkanski, Y., Fuzzi, S., Horth, J., Moortgat, G.K., Winterhalter, R., Myhre, C.E.L., Tsigaridis, K., Vignati, E., Stephanou, E.G., Wilson, J., 2005. Organic aerosol and global climate modelling: a review. Atmos. Chem. Phys. 5, 1053–1123.

Kaul, D.S., Gupta, T., Tripathi, S.N., Tare, V., Collett, J.L., 2011. Secondary organic aerosol: a comparison between foggy and nonfoggy days. Environ. Sci. Technol. 45, 7307–7313. http://dx.doi.org/10.1021/es201081d.

Khoder, M.I., 2002. Atmospheric conversion of sulfur dioxide to particulate sulfate and nitrogen dioxide to particulate nitrate and gaseous nitric acid in an urban area. Chemosphere 49, 675–684. http://dx.doi.org/10.1016/S0045-6535(02)00391-0.

Lim, Y.B., Tan, Y., Perri, M.J., Seitzinger, S.P., Turpin, B.J., 2010. Aqueous chemistry and its role in secondary organic aerosol (SOA) formation. Atmos. Chem. Phys. 10, 10521–10539. http://dx.doi.org/10.5194/acp-10-10521-2010.

Markowicz, K.M., Flatau, P.J., Quinn, P., Carrico, C.M., Flatau, M., Vogelmann, A., Bates, D., Liu, M., Rood, M.J., 2003. Influence of relative humidity on aerosol radiative forcing: an ACE-Asia experiment perspective. J. Geophys. Res. 108. http://dx.doi.org/10.1029/2002JD003066.

Matthew, B.M., Middlebrook, A.M., Onasch, T.B., 2008. Collection efficiencies in an Aerodyne Aerosol Mass Spectrometer as a function of particle phase for laboratory generated aerosols. Aerosol Sci. Technol. 42, 884–898.

Meng, Z.Y., Lin, W.L., Jiang, X.M., Yan, P., Wang, Y., Zhang, Y.M., Jia, X.F., Yu, X.L., 2011. Characteristics of atmospheric ammonia over Beijing, China. Atmos. Chem. Phys. 11, 6139–6151. http://dx.doi.org/10.5194/acp-11-6139-2011.

Middlebrook, A.M., Bahreini, R., Jimenez, J.L., Canagaratna, M.R., 2012. Evaluation of composition-dependent collection efficiencies for the Aerodyne Aerosol Mass Spectrometer using field data. Aerosol Sci. Tech. 46, 258–271.

Ng, N.L., Canagaratna, M.R., Zhang, Q., Jimenez, J.L., Tian, J., Ulbrich, I.M., Kroll, J.H., Docherty, K.S., Chhabra, P.S., Bahreini, R., Murphy, S.M., Seinfeld, J.H., Hildebrandt, L., Donahue, N.M., DeCarlo, P.F., Lanz, V.A., Prévôt, A.S.H., Dinar, E., Rudich, Y., Worsnop, D.R., 2010. Organic aerosol components observed in Northern Hemispheric datasets from Aerosol Mass Spectrometry. Atmos. Chem. Phys. 10, 4625–4641. http://dx.doi.org/10.5194/acp-10-4625-2010.

Ng, N.L., Canagaratna, M.R., Jimenez, J.L., Zhang, Q., Ulbrich, I.M., Worsnop, D.R., 2011. Real-time methods for estimating organic component mass concentrations from Aerosol Mass Spectrometer data. Environ. Sci. Technol. 45, 910–916. http://dx.doi.org/10.1021/es102951k.

Paatero, P., Tapper, U., 1994. Positive matrix factorization: a non-negative factor model with optimal utilization of error estimates of data values. Environmetrics 5, 111–126.

Quan, J., Zhang, Q., He, H., Liu, J., Huang, M., Jin, H., 2011. Analysis of the formation of fog and haze in North China Plain (NCP). Atmos. Chem. Phys. 11, 8205–8214. http://dx.doi.org/10.5194/acp-11-8205-2011.

Seinfeld, J.H., Pandis, S.N., 2006. Atmospheric Chemistry and Physics: From Air Pollution to Climate Change. Wiley, John & Sons, Incorporated, New York, p. 1203.

Shen, X., Lee, T., Guo, J., Wang, X., Li, P., Xu, P., Wang, Y., Ren, Y., Wang, W., Wang, T., Li, Y., Carn, S.A., Collett Jr., J.L., 2012. Aqueous phase sulfate production in clouds in eastern China. Atmos. Environ. 62, 502–511. http://dx.doi.org/10.1016/j.atmosenv.2012.07.079.

Shilling, J.E., Chen, Q., King, S.M., Rosenoern, T., Kroll, J.H., Worsnop, D.R., DeCarlo, P.F., Aiken, A.C., Sueper, D., Jimenez, J.L., Martin, S.T., 2009. Loading-dependent elemental composition of α-pinene SOA particles. Atmos. Chem. Phys. 9, 771–782.

Sorooshian, A., Murphy, S.M., Hersey, S., Bahreini, R., Jonsson, H., Flagan, R.C., Seinfeld, J.H., 2010. Constraining the contribution of organic acids and AMS m/z 44 to the organic aerosol budget: on the importance of meteorology, aerosol hygroscopicity, and region. Geophys. Res. Lett. 37, L21807. http://dx.doi.org/10.1029/2010gl044951.

Sun, J., Zhang, Q., Canagaratna, M.R., Zhang, Y., Ng, N.L., Sun, Y., Jayne, J.T., Zhang, X., Zhang, X., Worsnop, D.R., 2010. Highly time- and size-resolved characterization of submicron aerosol particles in Beijing using an Aerodyne Aerosol Mass Spectrometer. Atmos. Environ. 44, 131–140.

Sun, Y., Zhuang, G., Tang, A., Wang, Y., An, Z., 2006. Chemical characteristics of $PM_{2.5}$ and PM_{10} in haze-fog episodes in Beijing. Environ. Sci. Technol. 40, 3148–3155.

Sun, Y., Wang, Z., Dong, H., Yang, T., Li, J., Pan, X., Chen, P., Jayne, J.T., 2012. Characterization of summer organic and inorganic aerosols in Beijing, China with an Aerosol Chemical Speciation Monitor. Atmos. Environ. 51, 250–259. http://dx.doi.org/10.1016/j.atmosenv.2012.01.013.

Sun, Y.L., Wang, Z.F., Fu, P.Q., Yang, T., Jiang, Q., Dong, H.B., Li, J., Jia, J.J., 2013. Aerosol composition, sources and processes during wintertime in Beijing, China. Atmos. Chem. Phys. 13, 4577–4592. http://dx.doi.org/10.5194/acp-13-4577-2013.

Ulbrich, I.M., Canagaratna, M.R., Zhang, Q., Worsnop, D.R., Jimenez, J.L., 2009. Interpretation of organic components from Positive Matrix Factorization of aerosol mass spectrometric data. Atmos. Chem. Phys. 9, 2891–2918.

Volkamer, R., Jimenez, J.L., Martini, F.S., Dzepina, K., Zhang, Q., Salcedo, D., Molina, L.T., Molina, M.J., Worsnop, D.R., 2006. Secondary organic aerosol formation from anthropogenic VOCs: rapid and higher than expected. Geophys. Res. Lett. 33, L17811. http://dx.doi.org/10.1029/2006GL026899.

Wong, J.P.S., Lee, A.K.Y., Slowik, J.G., Cziczo, D.J., Leaitch, W.R., Macdonald, A., Abbatt, J.P.D., 2011. Oxidation of ambient biogenic secondary organic aerosol by hydroxyl radicals: effects on cloud condensation nuclei activity. Geophys. Res. Lett. 38, L22805. http://dx.doi.org/10.1029/2011gl049351.

Zhang, Q., Alfarra, M.R., Worsnop, D.R., Allan, J.D., Coe, H., Canagaratna, M.R., Jimenez, J.L., 2005. Deconvolution and quantification of hydrocarbon-like and oxygenated organic aerosols based on aerosol mass spectrometry. Environ. Sci. Technol. 39, 4938–4952. http://dx.doi.org/10.1021/es048568l.

Zhang, Q., Jimenez, J.L., Canagaratna, M.R., Allan, J.D., Coe, H., Ulbrich, I., Alfarra, M.R., Takami, A., Middlebrook, A.M., Sun, Y.L., Dzepina, K., Dunlea, E., Docherty, K., DeCarlo, P.F., Salcedo, D., Onasch, T., Jayne, J.T., Miyoshi, T., Shimono, A., Hatakeyama, S., Takegawa, N., Kondo, Y., Schneider, J., Drewnick, F., Weimer, S., Demerjian, K., Williams, P., Bower, K., Bahreini, R., Cottrell, L., Griffin, R.J., Rautiainen, J., Sun, J.Y., Zhang, Y.M., Worsnop, D.R., 2007a. Ubiquity and dominance of oxygenated species in organic aerosols in anthropogenically-influenced northern hemisphere mid-latitudes. Geophys. Res. Lett. 34, L13801. http://dx.doi.org/10.1029/2007GL029979.

Zhang, Q., Jimenez, J.L., Worsnop, D.R., Canagaratna, M., 2007b. A case study of urban particle acidity and its effect on secondary organic aerosol. Environ. Sci. Technol. 41, 3213–3219.

Zhang, Q., Tie, X., 2011. High solubility of SO_2: evidence in an intensive fog event measured in the NCP region, China. Atmos. Chem. Phys. Discuss. 11, 2931–2947. http://dx.doi.org/10.5194/acpd-11-2931-2011.

Zhang, H., Wang, S., Hao, J., Wan, L., Jiang, J., Zhang, M., Mestl, H.E.S., Alnes, L.W.H., Aunan, K., Mellouki, A.W., 2012a. Chemical and size characterization of particles emitted from the burning of coal and wood in rural households in Guizhou, China. Atmos. Environ. 51, 94–99. http://dx.doi.org/10.1016/j.atmosenv.2012.01.042.

Zhang, X., Liu, J., Parker, E.T., Hayes, P.L., Jimenez, J.L., de Gouw, J.A., Flynn, J.H., Grossberg, N., Lefer, B.L., Weber, R.J., 2012b. On the gas-particle partitioning of soluble organic aerosol in two urban atmospheres with contrasting emissions: 1. Bulk water-soluble organic carbon. J. Geophys. Res. 117, D00V16. http://dx.doi.org/10.1029/2012jd017908.

Zhang, Y., Schauer, J.J., Zhang, Y., Zeng, L., Wei, Y., Liu, Y., Shao, M., 2008. Characteristics of particulate carbon emissions from real-world Chinese coal combustion. Environ. Sci. Technol. 42, 5068–5073.